The correlation between the cylinder pressure and the ion current fitted with a Gaussian algorithm for a spark ignition engine fuelled with natural-gas –hydrogen blends

Zhongquan Gao, Bing Liu, Hui Gao, Xiangwen Meng, Chenglong Tang, Xiaomin Wu and Zuohua Huang

Proceedings of the Institution of Mechanical Engineers, Part D: Journal of Automobile Engineering 2014 228: 1480
originally published online 9 June 2014
DOI: 10.1177/0954407014533789

Original Article

Institution of MECHANICAL ENGINEERS
Journal of AUTOMOBILE ENGINEERING

Proc IMechE Part D:
J Automobile Engineering
2014, Vol. 228(12) 1480–1490

DOI: 10.1177/0954407014533789
pid.sagepub.com
SAGE

The correlation between the cylinder pressure and the ion current fitted with a Gaussian algorithm for a spark ignition engine fuelled with natural-gas–hydrogen blends

Zhongquan Gao, Bing Liu, Hui Gao, Xiangwen Meng, Chenglong Tang, Xiaomin Wu and Zuohua Huang

Abstract

An investigation was conducted of the ion current characteristics at various excess air ratios λ in a spark ignition engine fuelled with natural-gas–hydrogen blends. The Gaussian mathematical method was employed to fit the pure ion current signal without a spark tail generated by the ignition discharge. The cylinder pressure was recorded, and the Pauta criterion static threshold was used to deal with the outlier errors in the testing data for given cycles. The results show that the spark tail and the ion current can be separated by fitting the ion current with the Gaussian method, and the fitted pure ion current includes the flame-front stage and the post-flame stage. The timing with respect to the flame-front peak exhibits an irregular variation with λ. The maximum current in the flame-front stage increases with increasing λ.The timing of the maximum current in the post-flame stage occurs earlier at the stoichiometric ratio than at other air-to-fuel ratios. The correlation coefficient between the ion current in the post-flame stage and the pressure data treated with the Pauta criterion method increases. In addition, there are high correlation coefficients between the ion current and the pressure.

Keywords

Ion current, excess air ratios, natural-gas–hydrogen blends, Gaussian method

Date received: 11 September 2013; accepted: 9 April 2014

Introduction

Because of increasing concern about fuel shortage and exhaust emissions, much work has been carried out on electronic control techniques for spark ignition (SI) engine. The sensors in electronic control systems are typically utilized to obtain information about combustion in the cylinders. The ion current method using a spark plug as the sensor has attracted much attention owing to its rapid response, low cost and convenience.[1–6] There have been many reports on the applications of the ion current method to an online survey of SI engines. Daniels et al.[7] investigated partial-burn detection using an ionization current and noted that a light partial burn, which is difficult to observe using the pressure method, can be detected only by the ionization current. Abhijit et al.[8] observed the ion and pressure signals simultaneously under various operating conditions, and they found that the knock levels indicated by the ion currents are in reasonable agreement with those obtained from the pressure signals. Shamekhi and Graffari[9] correlated the ion current with the maximum cylinder pressure and the spark advance, and a fuzzy logic controller was developed for control of the optimum spark advance from the correlation results.

According to the generation mechanics, the ion current produced during combustion has three peaks: the

State Key Laboratory of Multiphase Flow in Power Engineering, Xi'an Jiaotong University, Xi'an, People's Republic of China

Corresponding author:
Xiaomin Wu, State Key Laboratory of Multiphase Flow in Power Engineering, Xi'an Jiaotong University, Xi'an, People's Republic of China.
Email: xmwu@mail.xjtu.edu.cn

Zhongquan Gao, State Key Laboratory of Multiphase Flow in Power Engineering, Xi'an Jiaotong University, Xi'an, 710049, People's Republic of China.
Email: gaozq@mail.xjtu.edu.cn

ignition peak, the flame-front peak and the post-flame peak. However, the spark tail from the ignition discharge with a voltage higher than 10 kV during the ignition process disturbs the ion current measured because the measurement circuit used for the ion current is connected to the ignition line and the spark plug. In particular, most SI engines operate with inductive ignition systems owing to their large ignition energy and reliability, and so the influence of the ignition discharge on the ion current is more extreme. Einewall et al.[10] detected the ion current at different exhaust gas recirculation (EGR) rates, and they found that the flame-front stage of the ion current was sometimes affected by noise from the ignition. Shimasaki et al.[11] reported that the ion current during the initial flame propagation was mixed with the current from the spark discharge and was hardly detected if the ignition discharge was long. Wu et al.[12] found that the ion current was disturbed by the ignition discharge when a spark plug was used as the sensor and that the ion current in both the flame-front stage and the post-flame stage were mixed with the spark tail. As it was considered that the influence of the spark tail on the ion current in the flame-front stage and the post-flame stage will lead to the loss of combustion information about the characteristic parameters of the ion current, several studies have been carried out on to reduce the influence of the ignition on the ionization current. Yoshiyama et al.[13] used a capacitance-type ignition system to reduce the duration of ignition and found that this method could guarantee the ion current quality only at low engine speeds. Saitzkoff et al.[14] de-noised the ion current signal with the wavelet threshold shrinkage method and reported that the wavelet threshold shrinkage method can be applied to de-noising the ion current signal in the post-flame stage. Gao et al.[15] separated the spark tail from the ion current using the blind source separation (BSS) method, and they found that a de-noised current could be extracted from a couple of measured currents. Although much research has been devoted to noise reduction on the basis of the mechanism and features of the ion current signal, few studies have been conducted on the application of mathematical methods to de-noising the ion current signal.

To achieve information on combustion in the engine cylinders using the ion current method, researchers have examined the correlation between the characteristic parameters of the ion current and the pressure in recent years. Badawy et al.[2] investigated the relationship between the combustion parameters and the ion current in a single-cylinder diesel engine, and they found that the ignition delay, the crank angle (CA) position where 50% of the total heat release occurs and the location of the peak cylinder pressure are all strongly dependent on the ion current at different engine speeds, loads, injection pressures and injection timings. Yoshiyama[16] detected the combustion quality in an SI engine using eight ion current electrodes installed around the cylinder gasket and observed that the ion current fraction accumulated is sensitive to the CA, the heat release and the mass fraction burned. Gao et al.[17] explored the relationship between the occurrence of the ion current timing detected by eight electrodes and the maximum pressure, and they found that the correlation coefficients between the average timing of the ion current and the maximum pressure are all greater than 0.9. Although the ion current obtained by extra measurement electrodes shows the correlation with the combustion parameters, cycle-by-cycle variations exist in the pressure owing to the complex combustion process in the engine. It is necessary to study the correlation between the characteristic pressure parameters and the ion current detected using a spark plug for a number of consecutive cycles.

Engines fuelled with a mixture of compressed natural gas (CNG) and hydrogen (20–50%) have attracted much interest in the last decade because of their lower cycle-by-cycle variations, better emission characteristics and higher fuel conversion efficiencies, when compared with those of gasoline engines.[18–24] In this paper, the characteristics of the ion current generated in an SI engine fuelled with a mixture of CNG–hydrogen blends are studied. To avoid the effect of the spark tail on the ion current, the Gaussian method is used to fit the pure ion current and the ignition signals. Correlations between the characteristic parameters of the ion current with the maximum pressure and the position for the maximum pressure are discussed, and a Pauta criterion static threshold is chosen to deal with the outlier errors in the testing data. Our results may help to establish a feasible correlation between the characteristic parameters of the pressure and those of the ion current of an SI engine fuelled with CNG–hydrogen blends.

Experimental set-up and procedures

The details of the CNG–hydrogen-fuelled engine and the ion current measurement circuit have been reported by Gao et al.[15] An HH368Q multi-fuel gasoline engine was used, and the ionization current measurement circuit was connected to the central electrodes of the spark plug by an electrical wire; then a high-voltage silicon stack, a bias power supply (400 V) and a grounded resistor (R_2 = 100 kΩ) were connected. Thus, the ionization current signals could be detected from both of the two ends of the grounded resistor when the engine was running.

Parameterization of the ion current with Gaussian functions

Klövmark et al.[25] proposed that the ion current can be fitted by two Gaussian functions since the ion current is similar to a Gaussian function. In this paper, considering that the ion current detected from the SI engine

cylinder includes three stages, namely the ignition stage, the flame-front stage and the post-flame stage, three Gaussian functions are adopted to fit the ion current. Thus, each stage of the ion current can be regarded as a function of the CA, and the total ion current is expressed as

$$I(\theta) = g_1(\theta) + g_2(\theta) + g_3(\theta) \tag{1}$$

where $g_i(\theta)$ is the ith Gaussian function in the three Gaussian functions, representing the ignition stage, the flame-front stage and the post-flame stage in the ion current in order.

The Gauss function can be expressed in the simple form[26]

$$g(\theta) = \alpha \exp\left[-\left(\frac{\theta-\beta}{\gamma}\right)^2\right] \tag{2}$$

and this is used for the calculations. The profile of equation (2) is shown in Figure 1, where α, β and γ denote the maximum value, the CA at the maximum value and the width respectively.

From equations (1) and (2), the fitted ion current function can be expressed as

$$\begin{aligned} I(\theta) &= g_1(\theta) + g_2(\theta) + g_3(\theta) \\ &= \alpha_1 \exp\left[-\left(\frac{\theta-\beta_1}{\gamma_1}\right)^2\right] + \alpha_2 \exp\left[-\left(\frac{\theta-\beta_2}{\gamma_2}\right)^2\right] \\ &\quad + \alpha_3 \exp\left[-\left(\frac{\theta-\beta_3}{\gamma_3}\right)^2\right] \end{aligned} \tag{3}$$

Since $g_1(\theta)$ is the function of the ignition stage, the interference of ignition can be excluded from the ion current, and thus the de-noised ion current can be obtained as

$$\begin{aligned} \hat{I}(\theta) &= g_2(\theta) + g_3(\theta) \\ &= \alpha_2 \exp\left[-\left(\frac{\theta-\beta_2}{\gamma_2}\right)^2\right] + \alpha_3 \exp\left[-\left(\frac{\theta-\beta_3}{\gamma_3}\right)^2\right] \end{aligned}$$

According to the definition of the Gaussian function and equation (3), β_1, β_2 and β_3 are the CA for the ignition stage, the CA for the flame-front stage and the CA for the post-flame stage respectively.

For a given data group (x_1, y_1), (x_2, y_2), …, (x_n, y_n) which accord with the Gaussian distribution, the Gaussian function is expressed as equation (2), where α, β and γ are unknown parameters which need to be obtained.

Employing natural logarithms for both the left-hand side and the right-hand side of equation (1) results in the equation

$$Y = Ax^2 + Bx + C \tag{5}$$

where

$$\begin{aligned} Y &= -\ln(y) \\ A &= \frac{1}{\lambda^2} \\ B &= -\frac{2\beta}{\lambda^2} \\ C &= \frac{\beta^2}{\lambda^2} - \ln(\alpha) \end{aligned}$$

Based on the theory of the least-squares method, A, B and C can be obtained from

$$\begin{bmatrix} \overline{x^2} & \overline{x} & 1 \\ \overline{x^3} & \overline{x^2} & \overline{x} \\ \overline{x^4} & \overline{x^3} & \overline{x^2} \end{bmatrix} \begin{bmatrix} A \\ B \\ C \end{bmatrix} = \begin{bmatrix} \overline{Y} \\ \overline{xY} \\ \overline{x^2 Y} \end{bmatrix} \tag{6}$$

where

$$\begin{aligned} \overline{x^j} &= \sum_{i=1}^{n} \frac{x_i^j}{n} \qquad (j = 1, 2, 3, 4) \\ \overline{x^m Y} &= -\sum_{i=1}^{n} \frac{x_i^m \ln(y_i)}{n} \qquad (m = 0, 1, 2) \end{aligned}$$

Finally, the three parameters can be found from

$$\begin{aligned} \alpha &= \exp\left(\frac{B^2}{4A} - C\right) \\ \beta &= -\frac{B}{2A} \\ \gamma &= \sqrt{\frac{1}{A}} \end{aligned} \tag{7}$$

Thus, α_i, β_i and γ_i (i = 1, 2, 3) were determined.

In this paper, the cftool toolbox of MATLAB software is selected, and the parameters α_i, β_i and γ_i and the Gaussian fitting curve are obtained rapidly.

The correlation coefficient R is adopted to correlate the characteristic parameters of the ion current and the pressure, and R can be determined from[27]

$$R(x, y) = \frac{1}{N} \sum_{i=1}^{N} \frac{(x_i - \bar{x})(y_i - \bar{y})}{\mathrm{SD}_x \, \mathrm{SD}_y} \tag{8}$$

where x_i and y_i are the specific values of the ion current and the pressure respectively in a combustion cycle, N is the total number of the cycles, $\bar{x}$ and $\bar{y}$ are the average values and SD_x and SD_y are the standard deviations. The interdependence between the ion current and the pressure can be evaluated from R.

Because of the cycle-by-cycle variations in the ion current caused by the complex combustion process, the ion current for some cycles is obviously abnormal. The outlier errors from abnormal data will affect the analysis of the ion current, and thus the Pauta criterion static threshold[21] is employed to treat the outlier errors in the testing data. The principle of the Pauta criterion is stated as follows.

For a given data group$(x_1, x_2, ..., x_n)$, the mean value δ of the dynamic noise is defined as

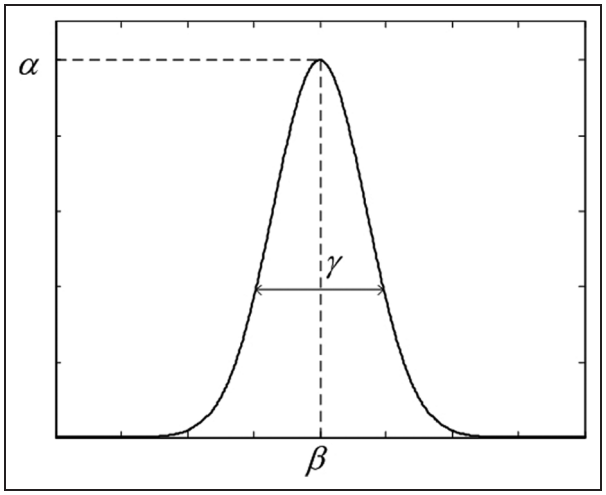

Figure 1. The Gaussian function and the meanings of its parameters.

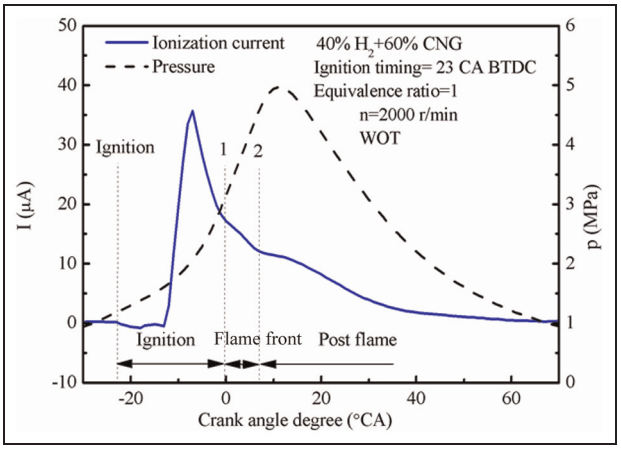

Figure 2. Typical ionization current and pressure.
H_2: hydrogen: CNG: compressed natural gas; CA: crank angle; BTDC: before top dead centre; WOT: wide-open throttle.

$$\delta = \sqrt{\frac{\sum_{i=1}^{n} (x_i - \bar{x})^2}{n = 1}} \tag{9}$$

where x_i represents the data on the ion current and the pressure in a combustion cycle, n is the total number of the cycles and $\bar{x}$ is the average value of the given data group. The normal data without outlier errors can be obtained using the Pauta criterion.

When the absolute value of the error is greater than 3δ ($|x_k - \bar{x}| > 3\delta$), the outlier errors x_k will be removed from the data group. This exclusion process is repeated until all the absolute errors are less than 3δ.

Results and discussion

Original ion current signal and de-noised ion current

As mentioned by Gao et al.,[15] the addition of the appropriate proportion of hydrogen to CNG will reduce the hydrocarbon concentration in the exhaust and will enhance the combustion process, and the CNG–hydrogen blend, which contains a volume fraction of 40% hydrogen, enables the engine to achieve a better performance and lower exhaust emissions. Thus a 60 vol % CNG–40 vol % hydrogen is adopted in this paper. Figure 2 illustrates the typical original ionization current signals measured from the cylinder chamber using a spark plug together with the de-noised ion current in the cylinders and the pressure respectively. The engine runs under the wide-open throttle (WOT) condition, at $\lambda = 1.0$, an ignition timing of 23° CA before top dead centre (BTDC) and an engine speed of 2000 r/min.

For the typical original current with three stages, the ignition stage (from the ignition point to the first transition, point 1), the flame-front stage (point 1 to the second transition, point 2) and the post-flame stage (after point 2) are presented in Figure 2, and the generation mechanisms of the three stages in the ion current have been given by Eisazadeh-Far et al.[28] From Figure 2, it can be seen that the flame-front stage is difficult to distinguish because the spark tail generated by ignition interfered with the ion current measured.

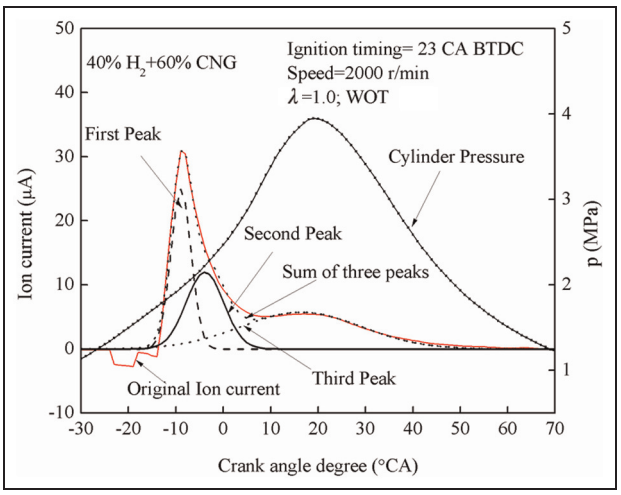

Figure 3. The results obtained from separating the peaks using the Gaussian function.
H_2: hydrogen: CNG: compressed natural gas; CA: crank angle; BTDC: before top dead centre; WOT: wide-open throttle.

The spark-tail noise easily interferes with the ion current, and it is too difficult to separate accurately the flame-front and post-flame stages from the ignition stage in the ion current for a number of cycles owing to the complex mechanism of the ion current and the intricate combustion in the cylinders.[13,15] This phenomenon implies that some combustion information included in the ion current in the cylinders may be missing, and thus we use the Gaussian method without considering the combustion factors which separate the ion current from the spark tail on the basis of the profile of the ion current measured in this paper. Figure 3 depicts the original ion current signal, the three separated current

Table 1. Parameters for Gaussian fitting results.

Engine speed (r/min)	Gaussian fitting results for three peaks								
	α_1	β_1	γ_1	α_2	β_2	γ_2	α_3	β_3	γ_3
2000	24.954	–8.9144	3.0266	12.002	–3.8903	5.5944	5.7114	16.417	17.935
3000	28.862	–11.428	3.2043	15.538	–5.6375	6.3233	12.084	15.385	22.227

peaks fitted by the Gaussian function, the sum of the three peaks and the pressure for a single cycle at an engine speed of 2000 r/min. The nine parameters to determine the three peaks in using the Gauss method are listed in Table 1.

A typical ion current has three peaks while the original ion current measured includes only two peaks. In the original ion current, the ignition stage and the flame-front stage are extremely mixed, and the post-flame stage cannot be distinguished clearly, because of interference by the spark tail. However, three distinct peaks corresponding to the ion current in the three stages can still be obtained with the Gaussian method although the original ion current has only two peaks. The positions of the three peaks calculated and shown in Figure 3 are reasonably consistent with the typical ion current reported in previous research on the ion current under the same experimental conditions. From the results of the Gaussian algorithm, the sum of the second peak (the flame-front stage) and the third peak (the post-flame stage) is the fitted ion current value without the occurrence of a spark tail.

Figure 4 presents the ion current fitted with the Gaussian method obtained from the second peak and the third peak in Figure 3, and it also displays the cylinder pressure. Therefore it is necessary to investigate further the relation between the ion current and the cylinder pressure. Thus the following four characteristic parameters of the fitted ion current and the two parameters of pressure are given, as shown in Figure 4: I_1, maximum flame-front ion current (μA); I_2, maximum post-flame ion current (μA); θ_1, CA for I_1 (deg CA after top dead centre (ATDC)); θ_2, CA for I_2 (deg CA ATDC); p_{max}, maximum pressure (MPa); θ_p, CA for $p_{\max}$ (deg CA ATDC).

In this paper, let $\theta_1 = \beta_2$ and $\theta_2 = \beta_3$, and thus I_1 and I_2 can be calculated from equations (3) and (4). θ_1 and θ_2 in Figure 4 can be obtained directly from Table 1, and the calculated I_1 and I_2 are 13.5 μA and 5.7 μA respectively. The value of I_2 in Figure 4 agrees well with the maximum value of the post-flame ion current in Figure 3. Figure 3 also shows the sum of the three peaks calculated with the Gaussian method and the original current measured during combustion. The sum of the three peaks is also consistent with the original ion current. The maximal absolute value of the difference between the sum of the three peaks and the original ion current is less than 1% of the original current. Moreover, the position interval between the

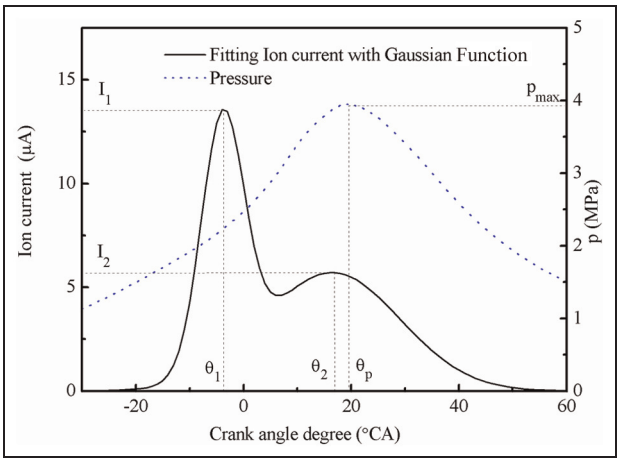

Figure 4. The ion current fitted with the Gaussian function. CA: crank angle.

maximum pressure and the second peak in Figure 4 is highly consistent with that in previous work.[29] These findings seems to show the feasibility of the Gaussian method in separating the ion current from the spark tail.

Original ion current and de-noised ion current versus excess air ratio

Figure 5 shows the average typical original ion current and pressure for 97 consecutive cycles at different excess air ratios under the WOT operation condition for an engine fuelled with the 60 vol % CNG–40 vol% hydrogen blend. The ignition timing is set to 23° CA BTDC at an engine speed of 2000 r/min, and to 27° CA BTDC at an engine speed of 3000 r/min, for all excess air ratios. As shown in Figure 5(a) and (c) with zoom insets at two engine speeds, nearly every ion current has only one peak because the three peaks of the ignition stage, the flame-front stage and the post-flame stage are extremely mixed owing to the interference by the spark tail generated by the ignition discharge. However, at $\lambda = 0.9$, 1.0 and 1.1 and an engine speed of 2000 r/min, the post-flame stage is distinguishable, and this is also true at $\lambda = 0.9$ and 1.0 and an engine speed of 3000 r/min. These results can be explained by assuming that, when the excess air ratio is approximately 1.0, the cylinder pressure is higher, as shown in Figure 5(b) and (d), leading to the generation of more ionized nitric oxide (NO) in the high-temperature zone,

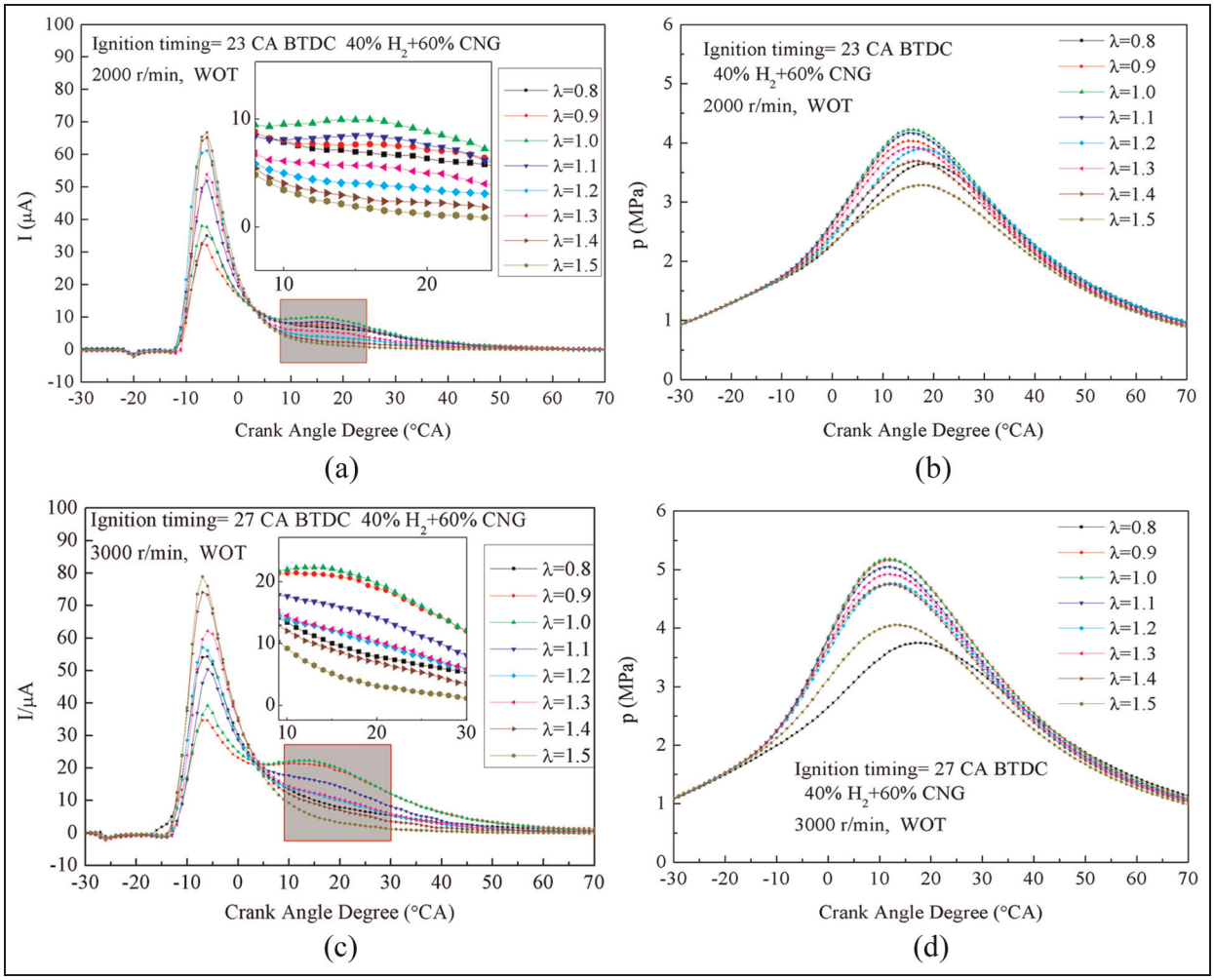

Figure 5. (a), (c) The original ion current and (b), (d) the pressure for different λ values at engine speeds of (a), (b) 2000 r/min and (c), (d) 300 r/min.
CA: crank angle; BTDC: before top dead centre; H_2: hydrogen: CNG: compressed natural gas; WOT: wide-open throttle.

which enhances the post-flame ion current. Moreover, the loss of some combustion information may occur when the original currents in the flame-front stage and the post-flame stage are mixed with the spark tail.

The average fitted ion currents based on the original currents of 97 consecutive cycles are illustrated in Figure 6(a) and (b). From the figure, it can be seen that, at $\lambda = 1.5$ and two engine speeds or at $\lambda = 0.8$ and an engine speed of 3000 r/min, the current has one peak and the post-flame stage is not obvious. The reason may be that the pressure under the above-mentioned conditions has lower peak values than those under other conditions, and thus the temperatures in the cylinder under these conditions are not sufficiently high for ionization of the NO fraction. In the ion current field, the one-peak phenomenon is usually used to diagnose a misfire. However, the fitted currents without interference by the spark tail are distinct and convenient for extraction of the characteristic parameters. These results confirm the reliability of the Gaussian method in extracting the pure ion current from the original ion current.

Figure 7 shows the characteristic pressure parameters θ_1 and θ_2 and the characteristic fitted current parameters I_1 and I_2 obtained from the data in Figure 6 at different excess air ratios. θ_1 shows small irregular fluctuations. I_1 increases with increasing λ. θ_2 increases under both lean- and rich-mixture conditions, and its minimum value occurs when $\lambda = 1.0$. I_2 decreases under both lean- and rich-mixture conditions. The current in the flame-front stage is related to the charged particles generated during the formation process of the flame kernel, and the flame kernel is dominated by the local air-to-fuel ratio and the gas flow around the narrow spark channel;[28] this leads to the fluctuations in θ_1 with a narrow range. Although the timing of I_1 fluctuates slightly, the calculated I_1 value increases with increasing λ, because I_1 is related to the charged particles generated during ignition and early propagation of the flame kernel, and thus I_1 is dominated by the dielectric constant of the gas in the spark plug gap. With increasing λ, the increased proportion of air increases the dielectric constant of the gas in the spark plug gap, resulting in a decrease in the spark tail. As the post-flame stage is

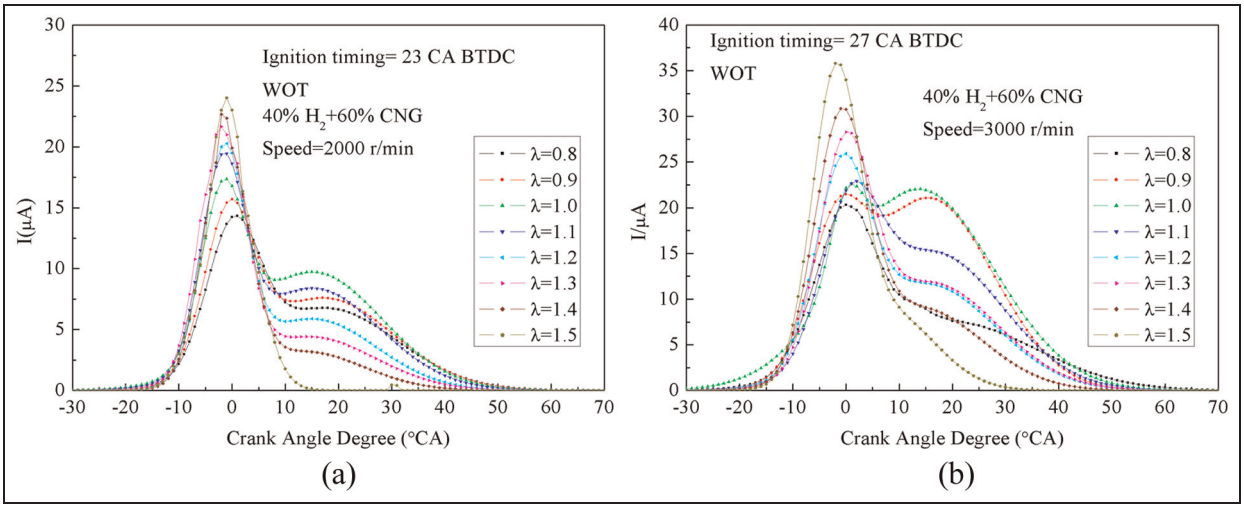

Figure 6. Fitted ion current for different λ values at engine speeds of (a) 2000 r/min and (b) 3000 r/min.
CA: crank angle; BTDC: before top dead centre; H_2: hydrogen: CNG: compressed natural gas; WOT: wide-open throttle.

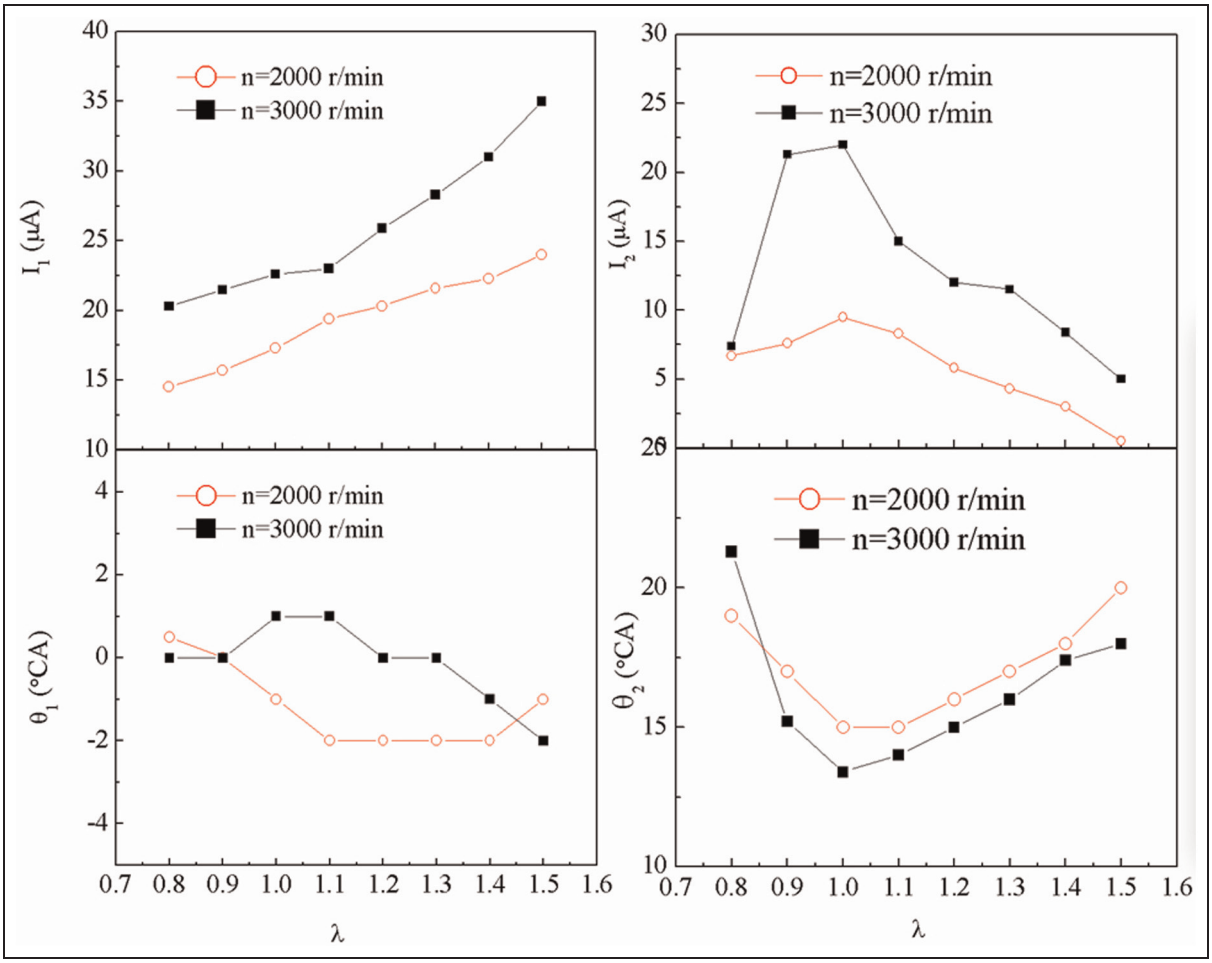

Figure 7. Characteristic parameters of the ion current versus λ.
CA: crank angle.

related to the thermal ionization process in the burned zone, the charged particles generated in the high-temperature zone dominate the current in this stage. It is well known that, at a given engine speed, θ_p is delayed when the excess air ratio is large or small, with the earliest θ_p occurring at $\lambda \approx 1.0$. p_{max} decreases when the

excess air ratio is large or small and its maximum value occurs at the stoichiometric ratio. Thus, θ_2 and I_2 have the same variations with increasing λ as θ_p and p_{max} respectively.

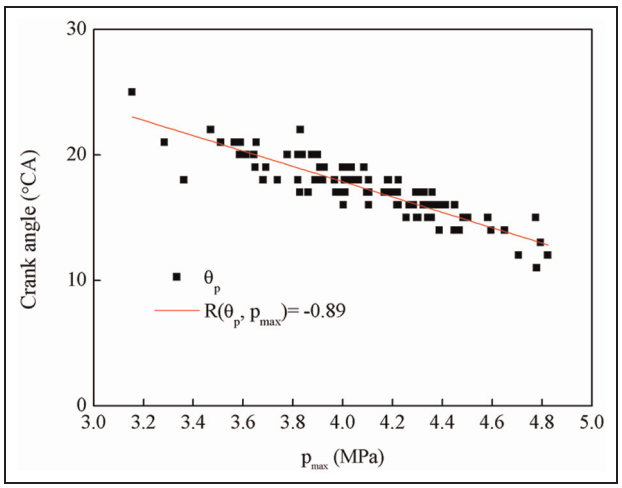

Figure 8. Interdependence between p_{max} and θ_p.
CA: crank angle.

The interdependence between the ion current and the pressure

Since the maximum pressure p_{max} and the timing θ_p of the maximum pressure are important variables in the estimation of the combustion quality, therefore much work has been performed on establishing the correlation between the characteristics parameters of the ion current and the pressure parameters p_{max} and θ_p. In this paper, the interdependence between the parameters of the ion current and the pressure parameters $p_{\max}$ and θ_p are investigated to obtains a more satisfactory correlation between the ion current de-noised by the Gaussian method and the pressure.

The results of the interdependence $R(\theta_p, p_{max})$ between p_{max} and θ_p are shown in Figure 8, and the operating conditions are the same as those in Figure 2 ($\lambda = 1.0$). It can be seen from the figure that $R(\theta_p, p_{max})$ is –0.89, indicating that p_{max} also strongly depends on θ_p. The interdependence between the four ion current parameters mentioned previously and θ_p for 97 cycles is illustrated in Figure 9 (with the same operating conditions as those in Figure 2), in which four least-squares fitting lines are given. The four correlation coefficients

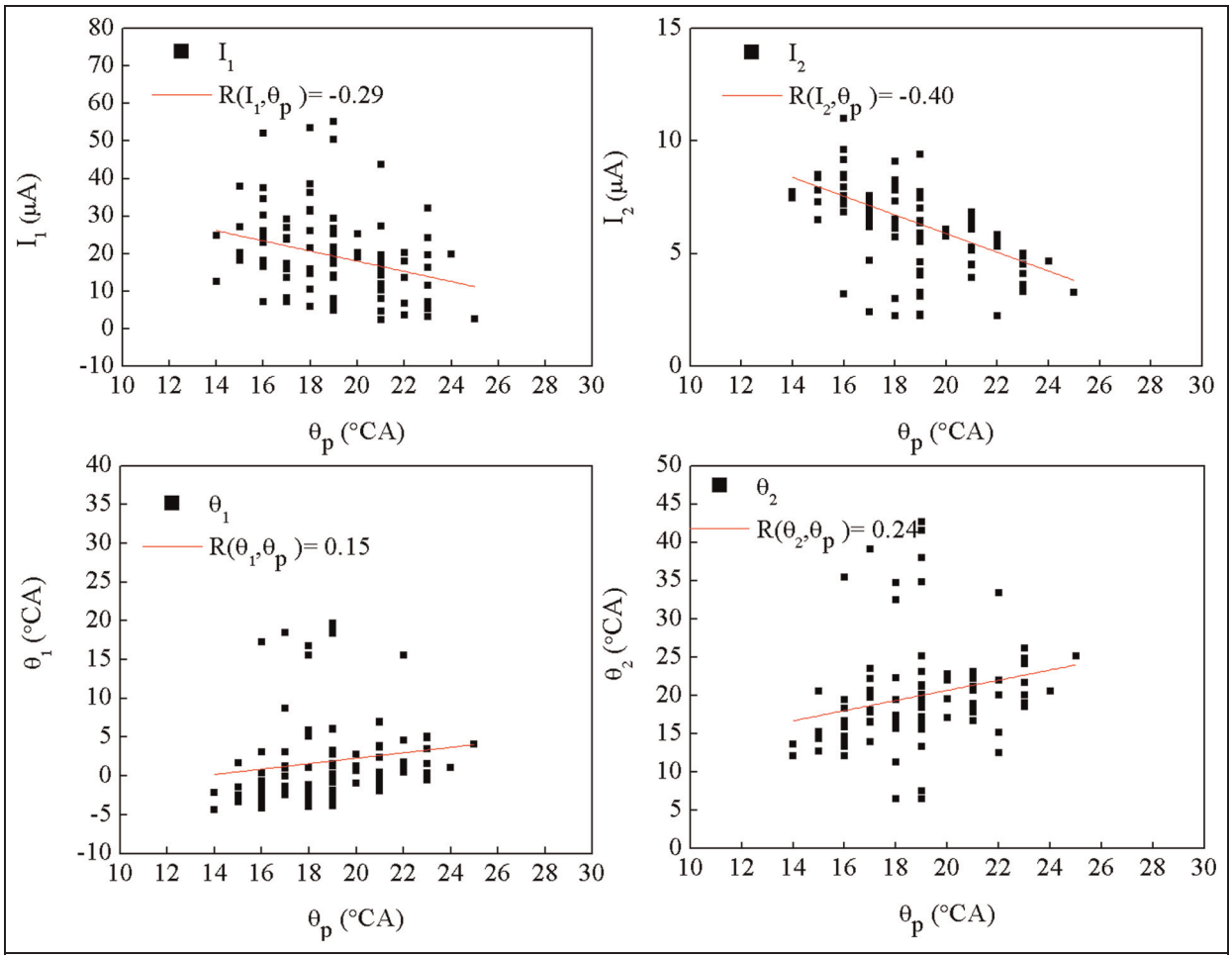

Figure 9. Interdependence between the ion current and θ_p.
CA: crank angle.

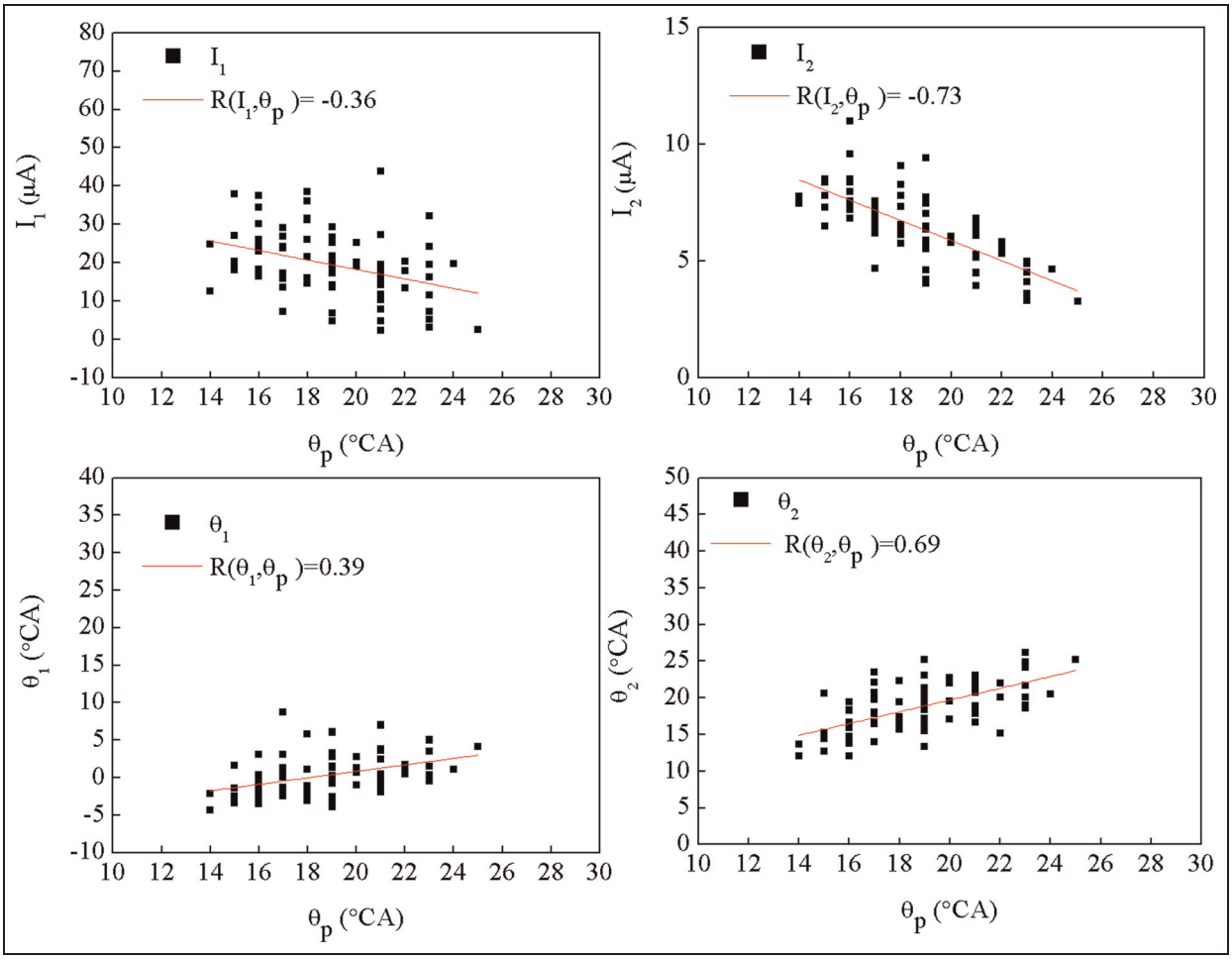

Figure 10. Interdependence between the ion current and θ_p, with the outlier errors removed by the Pauta criterion method. CA: crank angle.

are all smaller than 0.5, and the distributions of θ_1 and I_1 are irregular; however, for the other two parameters θ_2 and I_2, most data are concentrated around the fitted lines, as shown in Figure 9. These findings imply that there are abnormal points with gross errors in the measured data. To reduce the influence of the abnormal points, the Pauta criterion static threshold is used here to process the testing data in Figure 9. The parameters for the seven cycles with the outlier errors are removed by the Pauta criterion method and the parameters of the other 90 cycles without the outlier errors are shown in Figure 10. The two parameters θ_1 and I_1 of the flame-front stage versus θ_p also show abnormal points, and the two correlation coefficients related to I_1 and θ_1 are also smaller than 0.5. On the other hand, the data points of θ_2 and I_2 are more concentrated around the fitted lines than those in Figure 9 and the absolute values of the two correlation coefficients for I_2 and θ_2 are larger than 0.69 (see Figure 10). One reason for this could be that the maximum current in the flame-front stage is only related to the charged particles produced during the initial combustion in the cylinder. It is likely that the degree of interdependence between the ion current and the pressure is enhanced by the Pauta criterion method. However, compared with the correlation coefficient between p_{max} and θ_p, the interdependence of the parameters of the ion current and θ_p may not be sufficiently strong.

To establish a stronger relationship between the pressure and the ion current under given engine operation conditions, it is necessary to analyse further the ion current parameters. With the same operating conditions as those in Figure 2 ($\lambda = 1.0$ and an engine speed of 2000 r/min), the relationships between I_2,θ_2 and θ_p are presented in Figure 11, and θ_p is distributed in the range from 14° CA after top dead centre (ATDC) to 25° CA ATDC. The mean value of the ion current parameters corresponding to each CA for θ_p is calculated. The correlation coefficient between the mean value of I_2 and θ_p is –0.945, as shown in Figure 11(a), and that between the mean value of θ_2 and θ_p is 0.95, as shown in Figure 11(b). This indicates that the mean values of the ion current parameters in the post-flame stage are significantly dependent on the timing of the maximum pressure.

Conclusions

In this paper, we conducted an investigation on the ion current characteristics in an SI engine fuelled with a

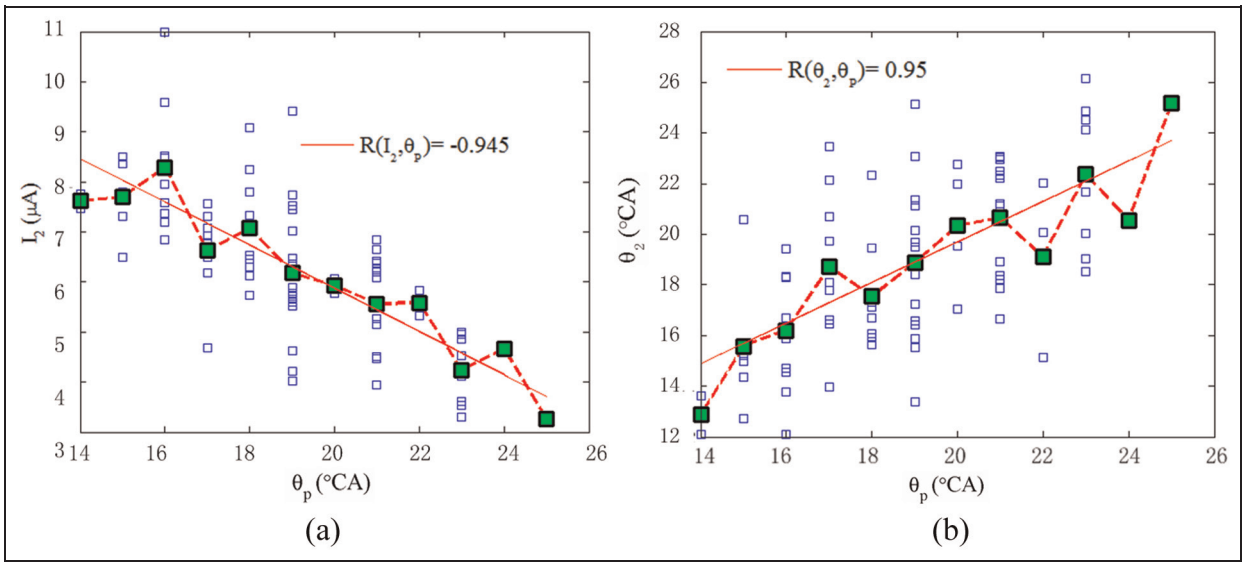

Figure 11. Relationship between the mean values of the ion current parameters and θ_p.
CA: crank angle.

CNG–hydrogen blend at various λ values. The Gaussian method was employed to fit the pure ion current signal without interference by the spark tail generated by the ignition discharge. The following conclusions can be drawn.

1. For the stoichiometric mixture, the measured ion current in the cylinder has an ignition stage, a flame-front stage and a post-flame stage. However, the measured ion currents have one or two peaks at other excess air ratios owing to interference by the spark tail generated by the discharge.
2. The pure ion current without interference by the spark tail can be fitted by the Gaussian method. Most pure ion currents have a flame-front stage and a post-flame stage. θ_p for lean and rich mixtures decreases with increasing λ, and the minimum value occurs when $\lambda = 1.0$. p_{max} decreases for lean and rich mixtures, and the maximum value occurs at the stoichiometric ratio. θ_1 shows small fluctuations with λ while I_1 increases with increasing λ. θ_2 and I_2 show the same variation trends as θ_p and p_{max} respectively.
3. For the given data group of 97 cycles adopted in this paper, the relationship between the pressure parameters and the ion current parameters is not obvious. The data for 90 cycles without the outlier errors removed by the Pauta criterion method are suitable for analysis. I_1 and θ_1 are just related to the ions and electrons generated during initial combustion in the cylinder. The ion current parameters of the post-flame stage depend significantly on the two pressure parameters.
4. The correlation between the average values of I_2 and θ_2 for each CA and θ_p is obtained, and the absolute correlation coefficients are higher than 0.9.

Funding

This work was supported by the National Natural Science Foundation of China (grant number 51306143 and grant number 51176150) and by the Fundamental Research Funds for the Central Universities (grant number: xjj2013001).

Declaration of conflict of interest

The authors declare that there is no conflict of interests regarding the publication of this article.

References

1. Zheng S, Zhang X and Shen Z. Study on cycle-by-cycle variations of ion current integral and pressure in spark ignition engine. In: *2011 international conference on electronic and mechanical engineering and information technology*, Harbin, Heilongjiang, People's Republic of China, 12–14 August 2011, pp. 3404–3407. New York: IEEE.
2. Badawy T, Rai N, Singh J et al. Effect of design and operating parameters on the ion current in a single-cylinder diesel engine. *Int J Engine Res* 2011; 126: 601–614.
3. Saikaly K. Preventive knock protection technique for stationary SI engines fuelled by natural gas. *Fuel Processing Technol* 2010; 91(6): 641–652.
4. Zhong Z et al. Detection of knocking by wavelet transform using ion current. In: *2009 4th international conference on innovative computing, information and control*, Kaohsiung, Republic of China, 7–9 December 2009, pp. 1566–1569. New York: IEEE.
5. Shamekhi AH and Ghaffar A. Fuzzy control of spark advance by ion current sensing. *Proc IMechE Part D: J Automobile Engineering* 2007; 221(3): 335–342.
6. Wu X, Li K and Jiang D. Investigation of air–fuel ratio control using ionic current signal. *Proc IMechE Part D: J Automobile Engineering* 2007; 221(9): 1139–1146.

7. Daniels C, Zhu GG and Winkelmen J. Inaudible knock and partial-burn detection using in-cylinder ionization signal. SAE paper 2003-01-3149, 2003.
8. Abhijit A, Naber J and George G. Ionization signal response during combustion knock and comparison to cylinder pressure for SI engines. SAE paper 2008-01-0981, 2008.
9. Shamekhi AH and Graffari A. Ion current simulation during the post flame period in SI engines. *Iran J Chem Chem Engng* 2005; 24(2): 51–58.
10. Einewall P, Tunestål P and Johansson B. The potential of using the ion-current signal for optimizing engine stability – comparisons of lean and EGR (stoichiometric) operation. SAE paper 2003-01-0717, 2003.
11. Shimasaki Y, Maki H, Sakaguchi J et al. Study on combustion monitoring system for Formula One engines using ionic current measurement. SAE paper 2004-01-1921, 2004.
12. Wu X, Gao Z, Jiang D and Huang Z. Experimental investigation of the effect of electrodes on the ionization current during combustion. *Energy Fuels* 2008; 22(5): 2941–2947.
13. Yoshiyama S, Tomita E and Hamamoto Y. Fundamental study on combustion diagnostics using a spark plug as ion probe. SAE paper 2000-01-2828, 2000.
14. Saitzkoff AM, Reinmann R, Mauss F and Glavmo M. In-cylinder pressure measurements using the spark plug as an ionization sensor. SAE paper 970857, 1997.
15. Gao Z, Wu X, Gao H et al. Investigation on characteristics of ionization current in a spark-ignition engine fueled with natural gas–hydrogen blends with BSS de-noising method. *Int J Hydrogen Energy* 2010; 35(23): 12 918–12 929.
16. Yoshiyama S. Detection of combustion quality in a production SI engine using ion sensor. SAE paper 2010-01-2255, 2010.
17. Gao Z, Wu S, Huang Z et al. The interdependency between the maximal pressure and ion current in a spark-ignition engine. *Int J Engine Res* 2013; 14(4): 320–332.
18. Hu E, Huang A, He J et al. Experimental and numerical study on laminar burning characteristics of premixed methane–hydrogen–air flames. *Int J Hydrogen Energy* 2009; 34(11): 4876–4888.
19. Ma F, Wang Y, Liu H et al. Effects of hydrogen addition on cycle-by-cycle variations in a lean burn natural gas spark-ignition engine. *Int J Hydrogen Energy* 2008; 33(2): 823–831.
20. Thurnheer T, Soltic P and Dimopoulos Eggenschwiler P. S.I. engine fuelled with gasoline, methane and methane/hydrogen blends: heat release and loss analysis. *Int J Hydrogen Energy* 2009; 34(5): 2494–2503.
21. Porowski R and Teodorczyk A. Experimental study on DDT for hydrogen–methane–air mixtures in tube with obstacles. *J Loss Prevention Process Ind* 2013; 26(2): 374–379.
22. Salzano E, Cammarota F, Di Benedetto A and Di Sarli V. Explosion behavior of hydrogen–methane/air mixtures. *J Loss Prevention Process Ind* 2012; 25(3): 443–447.
23. Day MS, Gao X and Bell JB. Properties of lean turbulent methane–air flames with significant hydrogen addition. *Proc Combust Inst* 2011; 33(1): 1601–1608.
24. Shoshin Y, Bastiaans RJM and de Goey LPH. Anomalous blow-off behavior of laminar inverted flames of ultra-lean hydrogen–methane–air mixtures. *Combust Flame* 2013; 160(3): 565–576.
25. Klövmark H, Rask P and Forssell U. Estimating the air/fuel ratio from Gaussian parameterizations of the ionization currents in internal combustion SI engines. SAE paper 2000-01-1245, 2000.
26. Eriksson L and Nielsen L. Ionization current interpretation for ignition control in internal combustion engines. *Control Engng Practice* 1997; 5(8): 1107–1113.
27. Zheng J, Huang Z, Wang J et al. Effect of compression ratio on cycle-by-cycle variations in a natural gas direct injection engine. *Energy Fuels* 2009; 23: 5357–5366.
28. Eisazadeh-Far K, Parsinejad F, Metghalchi H and Keck JC. On flame kernel formation and propagation in premixed gases. *Combust Flame* 2010; 157(12): 2211–2221.
29. Rivara N, Dickinson PB and Shenton AT. A neural network implementation of peak pressure position control by ionization current feedback. *Trans ASME, J Dynamic Systems, Measmt, Control* 2009; 131(5): 051003.

Appendix 1

Notation

p_{max}	maximum pressure
θ	crank angle
θ_p	crank angle for maximal pressure
λ	excess air factor

Abbreviations

ATDC	after top dead centre
BSS	blind source separation
BTDC	before top dead centre
CA	crank angle
CNG	compressed natural gas
EGR	exhaust gas recirculation
WOT	wide-open throttle